

# Holocene changes in moisture source and temperature revealed by the oxygen isotopic composition of fossil *Daphnia ephippia* in Sierra Nevada, southern Spain

Charo López-Blanco<sup>a,\*</sup>, Antonio García-Alix<sup>b</sup>, Isabel Sánchez-Almazo<sup>b</sup>, Gonzalo Jiménez-Moreno<sup>a</sup>, R.Scott Anderson<sup>c</sup>

<sup>a</sup> Department of Stratigraphy and Paleontology, University of Granada 18071 Granada, Spain

<sup>b</sup> Centro de Instrumentación Científica (CIC), University of Granada 18071 Granada, Spain

<sup>c</sup> Environmental Programs, School of Earth & Sustainability, Northern Arizona University, Flagstaff, AZ 86011, USA

## ARTICLE INFO

### Keywords:

Stable isotopes

$\delta^{18}\text{O}$

Chitin, precipitation source effect

Temperature, paleohydrology

## ABSTRACT

The study of oxygen isotopes in chitin and its use as a paleoclimatic proxy is still under development. The low oxygen content of chitin and the low sample weight of fossils have hindered this research topic, even though there is evidence of a strong correlation between the oxygen isotopic composition of chitin and the isotopic composition of the host water. In order to further this research we present a paleoclimatic reconstruction based on  $\delta^{18}\text{O}$  of cladoceran remains from the lake sediments of Laguna de Río Seco, Sierra Nevada, Spain. Here, modern water isotopic data were used as a modern analogue to establish an important influence on evaporative enrichment as the ice-free season advances. The oxygen isotope signal from *Daphnia* resting eggs was used as a proxy for autumn snapshots of the water isotopic composition at millennial time scales. Long-term changes were controlled by the moisture source and the summer insolation. Between deglaciation and 4.2 kyr BP,  $\delta^{18}\text{O}$  measurements exhibited generally depleted values only interrupted by a peak at  $\sim 7.2$  kyr BP, concurrent with a temperature maximum inferred from earlier quantitative reconstructions. A predominantly Atlantic moisture source and changes in the evaporation related to seasonality explained the isotopic variability at that time. From 4.2 kyr BP onwards, a notable enrichment in this isotopic signal occurred, which was consistent with greater influence of a Mediterranean precipitation source and higher evaporation at lower lake levels. This new isotope record provides a unique application of paleoclimates from cladocerans, which goes beyond the taxonomic and numerative methodology traditionally used in subfossil cladoceran analysis.

## 1. Introduction

Oxygen isotopes have become an essential tool used to reconstruct paleoenvironments in paleoecological studies, as they can provide information about past temperatures but also about distinct processes affecting the water cycle (Leng et al., 2006). The technique has been extensively applied to inorganic material – both biogenic and authigenic minerals – incorporated into lacustrine deposits (Leng and Marshall, 2004), but its application to certain organic compounds is still under development (Holtvoeth et al., 2019). For example, in the cellulose of aquatic plants, a constant enrichment with respect to the source water of  $\sim 27\text{--}28\text{‰}$  has been observed, which is independent of temperature (Yakir, 1992), plant species, and photosynthetic pathway (Epstein et al.,

1977; Sternberg and DeNiro, 1963; Sternberg et al., 1984, 1986). This well-established relationship has provided climate and lake-basin reconstructions based on isotopic records of aquatic cellulose in a wide variety of ecosystems (Beuning et al., 2002, 1997; Liu et al., 2023; Street-Perrott et al., 2018). In other organic components, such as chitin, this approach has been less explored. Wooler et al., (2004) were the first to examine the relationship of  $\delta^{18}\text{O}$  on chironomid head capsules and lake water and found similar results (isotopic enrichment of  $\sim 28\text{‰}$ ) to those reported for cellulose. Later on, other studies such as Chang et al., (2018), Lasher et al., (2017), Mayr et al. (2015), van Hardenbroek et al. (2012), and Verbruggen et al., (2011) also found a high correlation between the oxygen isotopic composition of chitin and the isotopic composition of the host water. Most of the recent advances were

\* Corresponding author.

E-mail address: [charolopezb@ugr.es](mailto:charolopezb@ugr.es) (C. López-Blanco).

<https://doi.org/10.1016/j.catena.2025.108984>

Received 9 October 2024; Received in revised form 14 March 2025; Accepted 22 March 2025

Available online 31 March 2025

0341-8162/© 2025 The Authors. Published by Elsevier B.V. This is an open access article under the CC BY license (<http://creativecommons.org/licenses/by/4.0/>).

summarized in van Hardenbroek et al. (2018).

Chitin is one of the most abundant polysaccharides in nature and is a major component of organisms like crustaceans, insects, fungi, and algae. Chitinous invertebrate remains are ubiquitous in aquatic environments, and both exoskeleton fragments and resting stages of insect orders such as Diptera (e.g. chironomids) or crustaceans (e.g. cladocerans) are commonly found in lake sediments (van Hardenbroek et al., 2018). In cladocerans, Verbruggen et al., (2011) found a strong and positive correlation between the oxygen isotope composition of their resting eggs (ephippia) and the host water ( $r = 0.94$ ;  $p < 0.01$ ). However, even though this chitinous material can be considered as a proxy for the  $\delta^{18}\text{O}$  of the water, very few studies have measured the oxygen isotopic record of chitin over time in cladocerans. Available evidence suggests that  $\delta^{18}\text{O}$  in chitin may be used to track past climate variability; however, more laboratory experiments are needed to better constrain the effect of temperature on oxygen isotope fractionation (Schilder et al., 2015). This young research field has been explored further in chironomid fossils, where some studies have been published on the methodology, fractionation aspects, and down-core records (Chang et al., 2016; Griffiths et al., 2010; Heiri et al., 2012; Raposeiro et al., 2024; Verbruggen et al., 2010b, 2010a). In cladocerans, one of the few contributions was recently published by Edgerton et al., (2024), who measured the stable oxygen isotopes from head capsules of chironomids and cladoceran ephippia and found similar temporal variability throughout the record. The inferred temperatures based on the  $\delta^{18}\text{O}$  of chitin in their study were broadly consistent with paleotemperatures at boreal locations and demonstrated the high potential of this poorly developed approach.

Oxygen commonly makes up 30 % of the elemental weight of cladoceran ephippia and chironomid head capsules, respectively (van Hardenbroek et al., 2018). Thus, several hundreds of chitinous remains must be hand-picked for each  $\delta^{18}\text{O}$  measurement, which can partially explain the poor development of the technique in comparison with more abundant elements such as carbon ( $\delta^{13}\text{C}$ ) (40–50 % of element weight) (Frossard et al., 2014; Perga, 2010; Perga and Gerdeaux, 2006; Schilder et al., 2017). Moreover, this polysaccharide has glucosamine or N-acetylglucosamine with nitrogen as a building block (Janssen et al., 2017) and a nitrogen content of ca. 7 % (Tracey, 1955). The oxygen isotopic analysis of nitrogen-rich samples implies certain methodological complications for the separation and detection of ions in the mass spectrometer. Chitin (and other nitrogen-rich samples) must be converted into gas by pyrolysis prior to the mass spectrometer analyses. As both  $\text{N}_2$  and  $\text{CO}$  are formed in the reactor during pyrolysis, tailing  $\text{N}_2$  peaks could be collected during the isotopic analysis of  $\text{CO}$  because both have the same mass, thus affecting the accuracy and precision of the measured oxygen isotopes (Brodie et al., 2016). Therefore, methodological adaptations are required to achieve complete chromatographic separation of the peaks.

Here we present one of the first down-core records describing past changes based on the oxygen isotopic composition of cladoceran ephippia, based on the Holocene record from the Laguna de Río Seco (Sierra Nevada, Spain). Our aims are as follows: 1) To examine the main controls on the isotopic signal of fossil chitin in cladocerans by comparing the sedimentary signal with the modern meteoric framework at the study site and 2) To reconstruct key aspects affecting the water cycle that can explain the multicentennial changes detected in the chitin  $\delta^{18}\text{O}$  record by comparing the obtained isotopic signal with results from previous paleoenvironmental studies on the lake (e.g. Jiménez-Moreno et al., 2023a; López-Blanco et al., 2024; Toney et al., 2020). Given the complexity of factors affecting the isotopic composition of the water from this alpine lake at millennial scales, previous studies are essential to interpret the sedimentary signal obtained in fossil cladocerans. In addition to these contributions, we provided new methodological information (e.g. analytical standards, separation of N and CO peaks, sample size) that can help the future development of this proxy. The great advantage of this taxon-specific approach over bulk sedimentary

organic matter/carbonate is that it can provide specific information on habitats and/or seasons when organic remains are produced which can eventually imply sub-annual resolution. A lower risk of terrestrial contamination is a further advantage of this material over cellulose and/or silica (Heiri et al., 2012).

## 2. Study site and the regional setting

Laguna de Río Seco (LdRS) is located in the southeastern Iberian Peninsula which is characterized by a typical Mediterranean climate with minimal annual precipitation. Summers are dry, especially during July and August (Fig. 1). Most of the annual precipitation comes from the Atlantic Ocean and is influenced by changes in the North Atlantic Oscillation (NAO), particularly in winter (Araguas-Araguas and Tejero, 2005). However, from the end of spring to autumn, humidity sourced from the Mediterranean Sea (WeMO) is a major component of the precipitation (Moreno et al., 2014). This influence is particularly high on the Mediterranean coast and the eastern part of the Iberian Peninsula (Araguas-Araguas and Tejero, 2005).

The total annual rainfall at LdRS is  $725 \pm 25$  mm, and because the lake is situated at 3020 m asl, most of the precipitation (75 %) falls as snow. The mean annual temperature is  $\sim 4.4$  °C, ranging from  $\sim 4$  °C in the coldest month to  $\sim 18$  °C in the warmest period (instrumental series data 1965–1993 Prado Llano-Alberque University at 2500 m asl;  $\sim 15$  km from the study site; Aemet Open data). The ice-free season usually lasts from June to October with high annual variability depending on the climatic conditions. LdRS has temporal inlets that during the ice-free season supply meltwater and rainwater to the basin (Fig. 1).

This small lake (0.42 ha) lies on mica schist bedrock and has a maximum depth of about 3 m. Physicochemical characteristics were described by Barea-Arco et al., (2001) and Morales-Baquero et al., (2006). The planktonic cladoceran community comprises *Daphnia pulex* (Pérez-Martínez et al. 2007), whereas the littoral community is mainly composed of *C. elegans*, *C. sphaericus*, and *A. quadrangularis* (López-Blanco et al., 2024).

## 3. Methods

### 3.1. Modern water samples and meteorological data

Modern water samples and meteorological data were collected from the study site to aid the interpretation of stable isotopes in paleoecological reconstructions. Surface water samples for hydrogen and oxygen isotope analysis were obtained during the ice-free season (June, July, August, September, and October) for four consecutive years (2020, 2021, 2022, 2023). Samples were collected in polyethylene bottles by refilling three times and capping the bottle underwater to remove any trapped air. After collection, samples were stored in a cooler and filtered in the lab using 0.45  $\mu\text{m}$  filters. A film of parafilm oil was used in each sample to prevent evaporation. They were then kept refrigerated until analysis at the Centro de Instrumentación Científica (CIC) at the University of Granada. Filtered water samples were analyzed for  $\delta^{18}\text{O}$  and  $\delta\text{D}$  using a Picarro L2140-i cavity ring-down spectroscopy (CDRS) laser instrument; where each sample was measured 6–10 times from a 2  $\mu\text{L}$  water injection. Repeated analysis of the standards (B2194, B2193, B2192) calibrated the data and gave a precision of  $\leq 0.02$  ‰ for  $\delta^{18}\text{O}$  and  $\leq 0.3$  ‰ for  $\delta\text{D}$ . Water isotopic data are reported in per-mill notation on the Vienna Standard Mean Ocean Water (‰ VSMOW) scale. To compare these data with the modern meteoric framework for Laguna de Río Seco, we also compiled data from the Global Network of Isotopes in Precipitation (GNIP; IAEA) to establish a local meteoric water line (LMWL) and modelled isotopic monthly values of meteoric water for Laguna de Río Seco using the Online Isotopes in Precipitation Calculator (OIPC, accessible at <https://wateriso.utah.edu>).

Data from air temperature were recovered from a HOBO TidbiT MX Temperature 400' Data Logger situated on the lake, which allowed

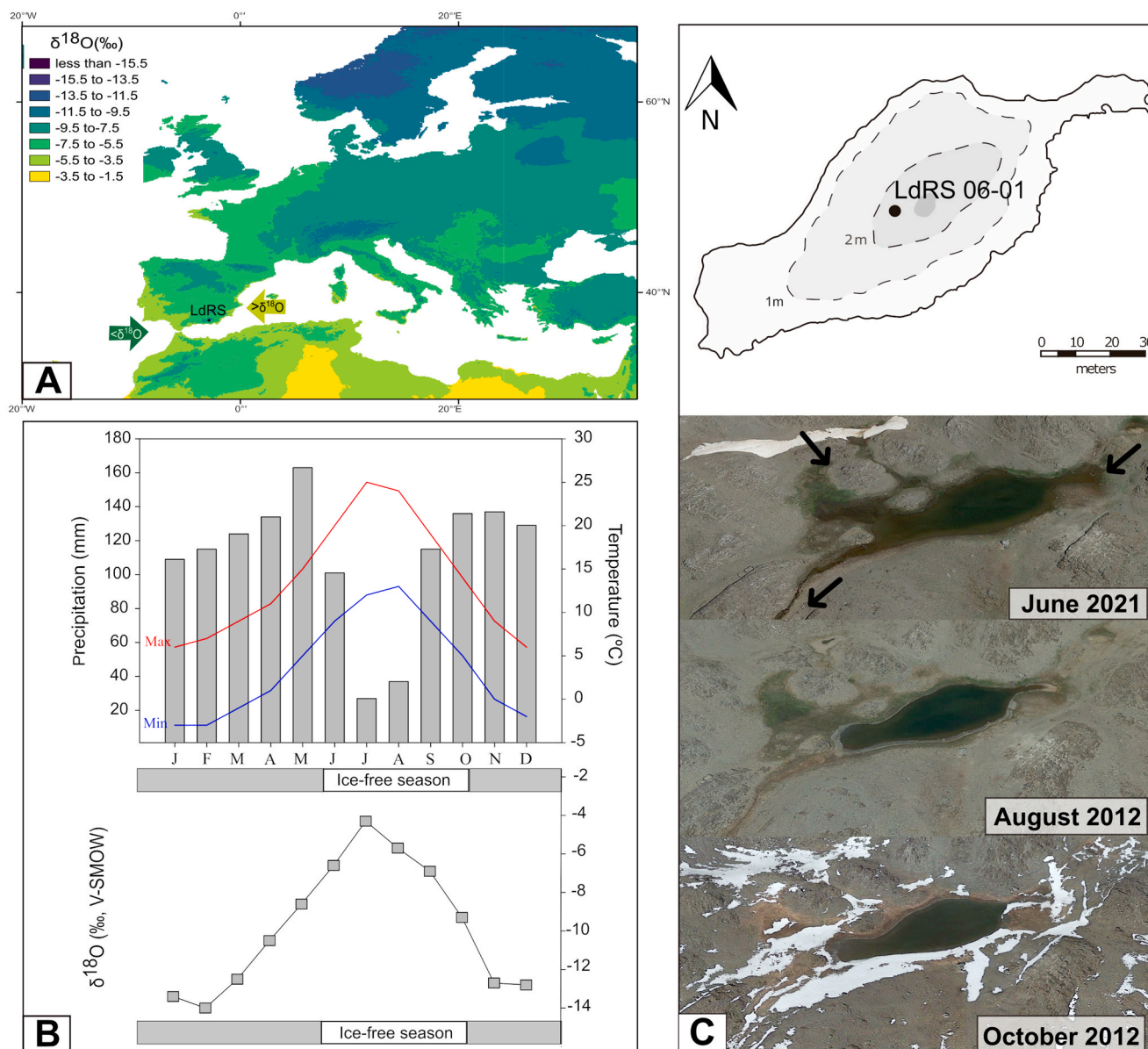


**Fig. 1.** Study site. A) General oxygen isotope composition of precipitation in Europe (based on Bowen and Revenaugh 2003; Bowen et al. 2005 downloaded from <https://wateriso.utah.edu>) and location of the Laguna de Río Seco (LdRS) in the southern part of the Iberian Peninsula. B) Average monthly temperature (maximum and minimum) and precipitation from the Pradollano Meteorological Station for the last 30 years (Agencia Estatal de Meteorología, AEMET) and estimation of the  $\delta^{18}\text{O}$  of precipitation at LdRS modeled by the online Isotopes in Precipitation calculator (OIPC 3.1) (grey squares). C) Bathymetry of the LdRS indicating the coring point (modified from García-Alix et al., 2020) and selected aerial photographs (<https://www.google.es/intl/es/earth/index.html>) showing the temporal inlets/outlets in the lake. Note that at the beginning of the ice-free season, several inlets drain water from the catchment (June 2021) and the lake becomes hydrologically closed as the ice-free season advances (i.e. August 2021).

remote temperature monitoring. This instrument recorded the temperature each hour during the four consecutive years (2020, 2021, 2022, 2023) and automatically computed the monthly average. From these data, the mean late spring temperature was calculated by considering the average data of May-June and was used to indicate the beginning of thawing.

### 3.2. Sediment sample collection

Selected sediment samples from a 150-cm sediment core (LdRS 06-01) spanning the last 21 cal kyr BP were used for cladoceran isotopic analysis. Details of this core were originally published in Anderson et al. (2011) and the chronology was modified in Jiménez-Moreno et al. (2023a). As prolonged exposure to strong chemicals can alter the

isotopic signal in chitin (Verbruggen et al. 2010a), our pretreatment only included water. Sediment samples were sieved at 100  $\mu\text{m}$  and ephippia from *Daphnia* and carapaces from *Chydorus sphaericus* were sorted out. Before isotopic analyses, *Daphnia* ephippia were digitally photographed and measured as shown in López-Blanco et al. (2024). Then, the ephippia and carapaces were meticulously rinsed several times with distilled water and brushed under a stereomicroscope in case of residues of mineral and/or organic matter attached to the surface. Carbonate coating of these subfossil materials is highly unlikely in this lake, as the lake lies on acidic rocks. Once cleaned with water, each ephippium was separated and picked using soft Insect Forceps (Fine Science Tools, 26029-19). Ephippia and carapaces were then loaded into pre-weighed silver cups (5 x 3.5 mm, INTEC Analysis Elements). Previously, it was determined that only samples containing > 0.4 mg of

cladoceran tissue displayed stable  $\delta^{18}\text{O}$  values in the IRMS, indicating that more than 1200 carapaces of *C. sphaericus* and approximately 120 ephippia of *Daphnia* were necessary to reach this amount in each sample. To obtain such a quantity of material, several consecutive samples from the sediment core were merged, which caused a loss in the temporal resolution of the data.

### 3.3. Stable isotope mass spectrometry

The cladoceran oxygen-isotope analyses were performed at the Laboratory of Stable Isotopes at the CIC-UGR using an EA IsoLink CNSOH connected to a Delta V Advantage IRMS via a ConFlo IV interface (Thermo Fisher Scientific).

The dried samples were weighed on a precision balance to pack  $0.5 \pm 0.05$  mg of sample into silver capsules and introduced into the pyrolysis column filled with glassy carbon using a Zero Blank Autosampler (Costech Analytical). Samples were pyrolyzed at  $1430^\circ\text{C}$ , and the resultant gases were separated using a chromatography column at  $45^\circ\text{C}$ . Chitin from cladoceran subfossils contains nitrogen and thus  $\text{N}_2$  gas is produced during high-temperature conversion (HTC). This  $\text{N}_2$  gas reacts with trace amounts of oxygen in the mass spectrometer source to form  $^{14}\text{N}^{16}\text{O}$  ( $m/z$  30), which creates isobaric interference with the  $^{12}\text{C}^{18}\text{O}$  peak ( $m/z$  30) of the sample. This interference results in less accurate  $\delta^{18}\text{O}$  values (Brodie et al., 2016). To improve the accuracy of the measurements, we ensured good chromatographic separation and diluted the nitrogen peak during the analysis using the dilution options of the ConFlo IV interface during the IRMS methods. Analytical uncertainties were  $\leq \pm 0.4$  ‰ based on repeat analyses of four international reference and nitrogen-rich standards (USGS42 Tibetan human hair, USFS43 Indian human hair, CBS Caribou Hoof Standard and KHS Kudu Horn Standard). Stable isotopic compositions were expressed in standard delta ( $\delta$ ) notation in ‰ relative to V-SMOW (Vienna Standard Mean Ocean Water). Once the results were obtained, a Mann-Kendall trend test (PAST software) was applied to isotope data to detect significant trends over the period of study.

## 4. Results

### 4.1. Modern isotopic variability

Surface water samples recovered during the ice-free season for LdRS fall below both the Global Meteoric Water line (GMWL,  $\delta^2\text{H} = 8\delta^{18}\text{O} + 10$ ), the Western Mediterranean Meteoric Water Line (WMMWL,  $\delta^2\text{H} = 8\delta^{18}\text{O} + 22$ ), and the modeled LMWL at LdRS ( $\delta^2\text{H} = 7.156\delta^{18}\text{O} + 5.6$ ) (Fig. 2). The mean values ( $n = 31$ ) were  $-4.4$  ‰ for  $\delta^{18}\text{O}$  and  $-37.9$  for  $\delta^2\text{H}$ . The maximum and minimum were  $-0.84$  ‰ and  $-9.4$  ‰ for  $\delta^{18}\text{O}$  and  $-18.9$  ‰ and  $-62.9$  ‰ for  $\delta^2\text{H}$ , respectively.

The seasonality of the oxygen isotope data of lake water is further explored in Fig. 2B, where the data exhibit a clear seasonal pattern in isotope enrichment as the summer advances, with minimum values in June-July and maximum in September-October. The average differences between maximum and minimum values were 5.89 ‰ in 2020, 6.28 ‰ in 2021, 5.01 ‰ in 2022 and 5.96 ‰ in 2023. Differences in absolute numbers were especially evident between 2020, as this year displayed more depleted values than the rest of the studied periods. In 2020, the late spring temperature (mean values from May and June) was also notably lower, with mean values of  $3.8^\circ\text{C}$  in comparison with  $5.7^\circ\text{C}$  and  $5.2^\circ\text{C}$  registered in 2022 and 2023, respectively (Fig. 2).

### 4.2. Oxygen isotopes in the fossil *Daphnia*

The *Daphnia* ephippia concentration in  $2\text{ cm}^3$  of sandy sediment from the bottommost part of the sedimentary core was low, with an average number of 25 ephippia in the Late Pleistocene (LP) and Early Holocene (EH) (Fig. 3). Concentrations slowly increased in the Middle Holocene (MH) and peaked around 5.5 cal kyr BP, with 200 ephippia per sample.

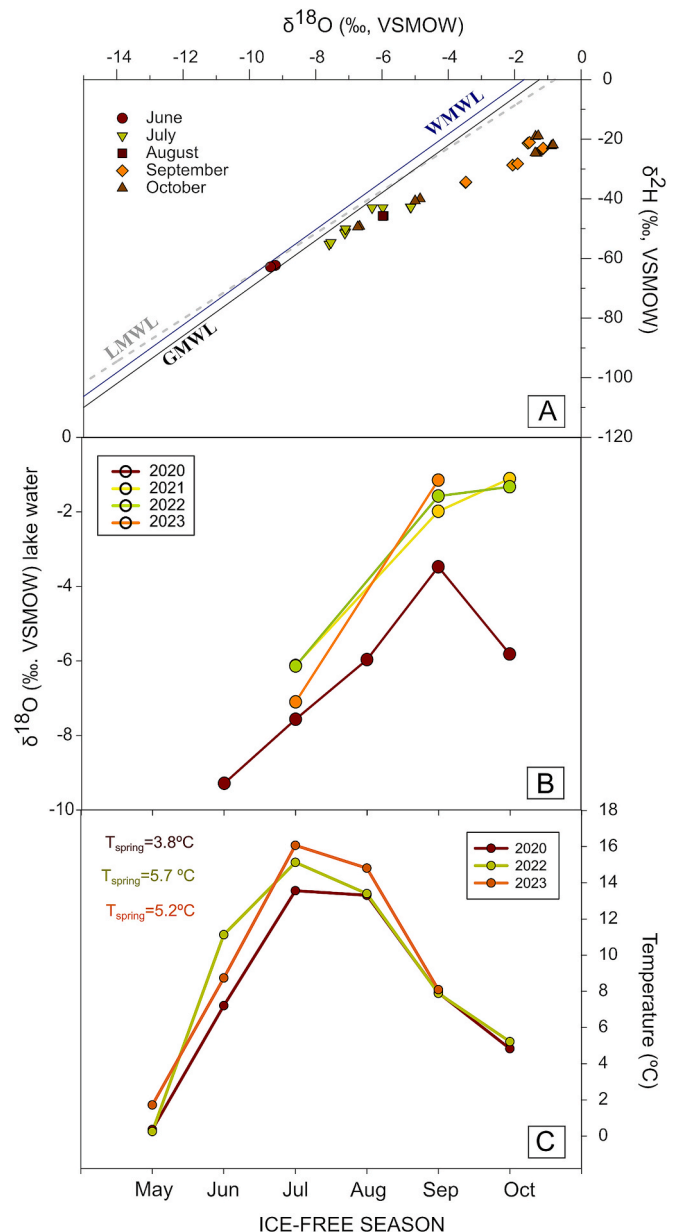


**Fig. 2.** (A) Scatter plots of  $\delta^2\text{H}_w$  versus  $\delta^{18}\text{O}_w$ , western Mediterranean Water Line (WMMWL), Global Meteoric Water Line (GMWL) and Local Meteoric Water Line (LMWL) (B) Temporal evolution of  $\delta^{18}\text{O}_w$  during the ice-free season in four consecutive years of sampling in the Laguna de Río Seco and (C) Variation of monthly air temperature ( $^\circ\text{C}$ ) during 2020, 2022 and 2023. Note that the spring (May-June average) temperature is indicated for each sampling year.

Thereafter they decreased toward the Late Holocene (LH), only interrupted by a peak in maximum abundance around 4.0 cal kyr BP, where around 400 ephippia were recovered per sample (Fig. 3). This material allowed us to obtain an oxygen isotope signal of *Daphnia* ephippia for the entire Holocene and part of the deglaciation *sensu lato*. The Mann-Kendall test showed a statistically significant increasing trend of oxygen isotopes over the studied period.  $\delta^{18}\text{O}$  of *Daphnia* ephippia showed mean values of  $+11.82$  ‰. The  $\delta^{18}\text{O}$  profile showed less positive values during the deglaciation with an increasing tendency toward the Middle Holocene. The most positive values reached about 7.3 cal kyr BP in the transition between the Early and Middle Holocene. After this period, there was a sharp depletion, and the oxygen isotope stratigraphy displayed the lowest values at  $\sim 6.5$  cal kyr BP. In the Late Holocene, especially after 4.2 cal kyr BP, oscillations occurred within a general

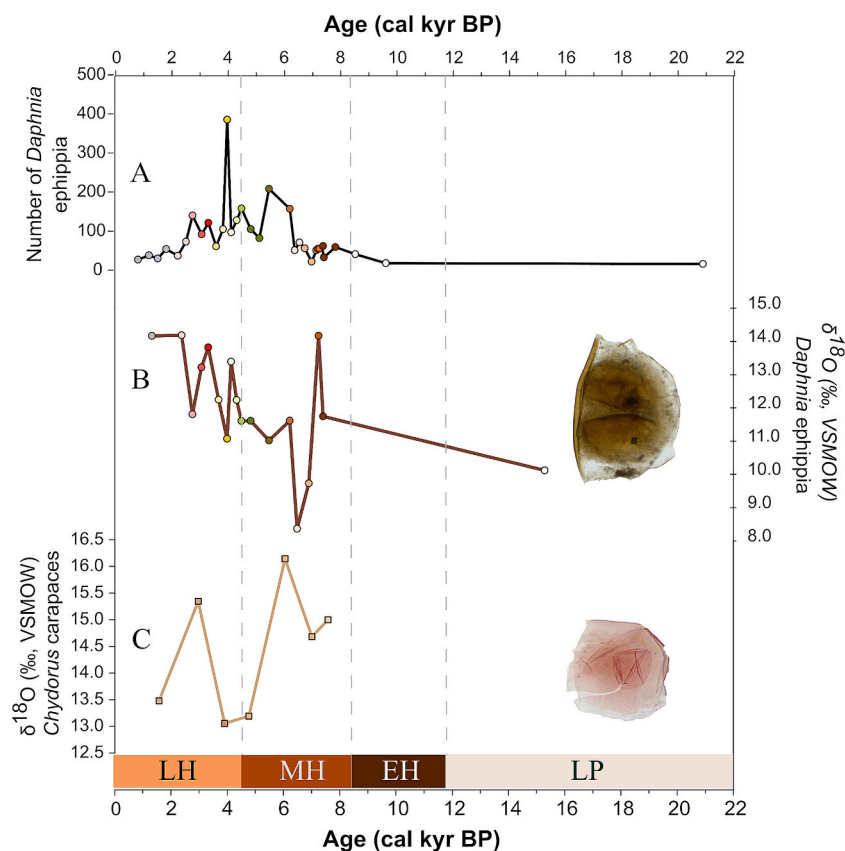


Fig. 3. (A) Number of *Daphnia* ehippia recovered from each sediment sample (2 cm<sup>3</sup>), (B) oxygen isotope stratigraphy ( $\delta^{18}\text{O}$ ) of *Daphnia* ehippia, and (C)  $\delta^{18}\text{O}$  of *Chydorus* carapaces for the LdRS06-01 sediment core.

tendency towards more positive values in the direction of the top of the sediment core.

The relatively smaller size and weight of *Chydorus* carapaces in comparison with *Daphnia* implied merging more samples to reach the required amount for isotope analysis. This issue resulted in insufficient measured depths to establish long-term tendencies throughout the Holocene and prevented comparisons with the stratigraphy of *Daphnia*, although values in *Chydorus* are nearly 2 ‰ higher than in *Daphnia*.

## 5. Discussion

### 5.1. Paleocological meaning of oxygen isotopes of *Daphnia* ehippia

In the contemporaneous lake, *Daphnia* ehippia are formed every year just before the beginning of the ice season (end September–October) as a mechanism of the species to persist in the sediment and hatch with the next thawing (Pérez-Martínez et al., 2007). Assuming a strong positive correlation between the oxygen-isotope ratio of host water ( $\delta^{18}\text{O}_w$ ) and invertebrate ehippia ( $\delta^{18}\text{O}_{\text{ehippia}}$ ) (Verbruggen et al., 2011; Wooller et al., 2004), we presume that the oxygen isotope signal in *Daphnia* resting eggs reflect early-autumn snapshots of the oxygen isotope values of the lake water. However, we have no certainty if the seasonal timing of ehippia production (and hence the period represented by *Daphnia*  $\delta^{18}\text{O}$  values) remained constant throughout the Holocene. If so, the oxygen isotope signal from *Daphnia* resting eggs in LdRS might provide early-autumn snapshots of the water isotopic composition at millennial scales, where each point would represent the autumn  $\delta^{18}\text{O}$  water average of hundreds of years.

The oxygen isotope composition of the water is largely affected by the lake paleohydrology, which depends on several factors including the moisture source, temperature or residence time. Traditionally, open lakes are considered to be subject to minimal evaporation, with the

isotope composition of the water usually reflecting the precipitation, both rainfall and snowfall, received in the catchment (Leng et al., 2006). LdRS exhibits a bimodal pattern of open then closed lake concerning the hydrology, with temporal inlets that drain water from the catchment at the beginning of the thawing (open lake  $\rightarrow$  short residence time), but as the ice-free season advances, the lake becomes a closed system when the inlets/outlets disappear (Fig. 1C). This fact explains why contemporaneous isotopic data were situated below the meteoric water lines and displayed a slope of 4.9 (Fig. 2), indicating a highly evaporated system (Craig, 1961). The shared seasonality pattern detected in all sampled years indicated enrichment in heavier isotopes as the ice-free season progressed (Fig. 2). Any effect of the summer rainfall, which is very scarce at these latitudes (Fig. 1B), is in general negligible compared with the evaporative concentration. However, it can eventually influence the isotopic composition as shown in depleted oxygen isotopic values in October 2020 (Fig. 2B). If occurring, summer/early autumn rainfall shows relatively enriched oxygen isotopic values, as it is mainly sourced by the Mediterranean moisture. In sedimentary records, however, other processes might come into play when considering changes over multiple millennia.

### 5.2. Paleohydrological reconstruction

#### 5.2.1. Before the 4.2 kyr event: Atlantic influence and changes in summer insolation (evaporation)

Understanding the controls of the oxygen isotopic composition of the water before reaching the lake is crucial for explaining the lake  $\delta^{18}\text{O}_{\text{ehippia}}$  sedimentary variations. Relatively low  $\delta^{18}\text{O}_{\text{ehippia}}$  in the bottom part of the sequence (Late Pleistocene–Early Holocene) (Figs. 3, 4) is consistent with the low inferred temperatures and low evaporation during deglaciation (Jiménez-Moreno et al., 2023a) (Fig. 4C) because fractionation during the first episodes of snow/ice melting onto liquid

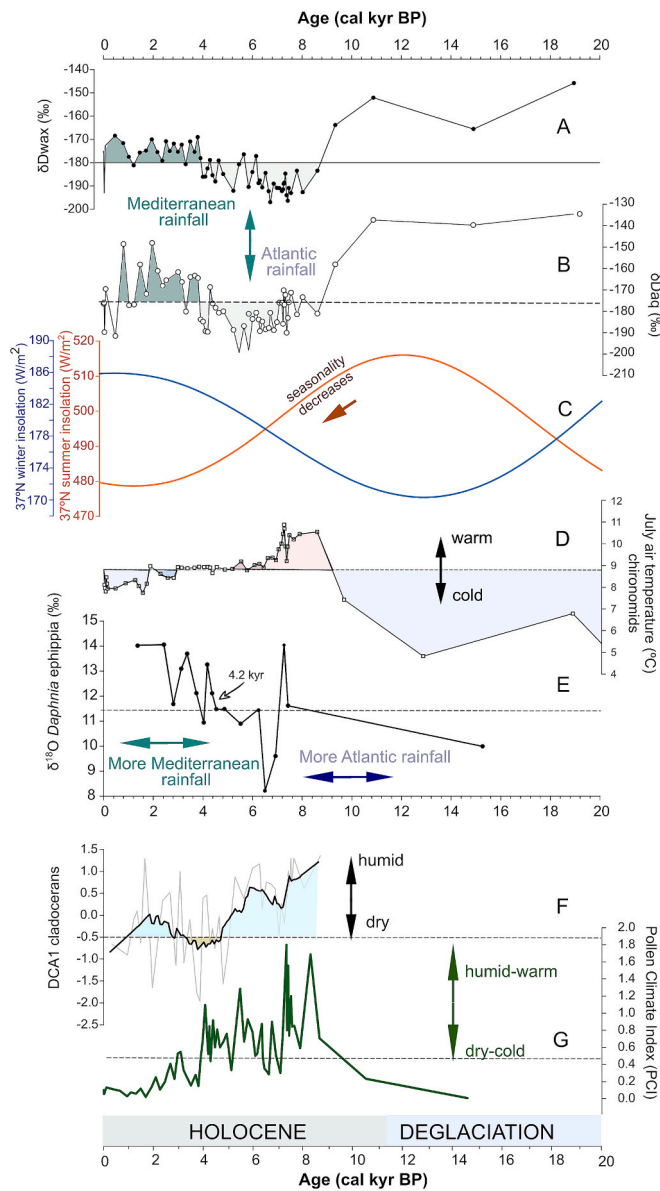


**Fig. 4.** Comparison of the oxygen isotope stratigraphy ( $\delta^{18}\text{O}$ ) of *Daphnia* ephippia (E) with selected proxies from the same LdRS06-01 core: (A) Hydrogen isotopic composition of the terrestrial C29 and C31 n-alkanes ( $\delta\text{D}_{\text{wax}}$ ) (Toney et al., 2020); (B) Hydrogen isotopic composition of the aquatic C23 and C25 n-alkanes ( $\delta\text{D}_{\text{aq}}$ ) (Toney et al., 2020); (C)  $37^\circ\text{N}$  mean monthly summer insolation obtained online (<https://vo.imcce.fr/insola/earth/online/earth/online/index.php>) from Laskar (2004); (D) July Air Temperature ( $^\circ\text{C}$ ) inferred from chironomid (Jiménez-Moreno et al., 2023a); (F) inferred lake-level changes from cladoceran subfossils (López-Blanco et al., 2024) and (G) Pollen Climate Index (PCI), calculated from Anderson et al., (2011). Temporal divisions (Deglaciation sensu lato and Early Holocene sensu lato) were performed in concordance with Jiménez-Moreno et al. (2023a).

water led to the depletion of  $\delta^{18}\text{O}$  (and 2H) in the liquid phase. As the temperature (Jiménez-Moreno et al., 2023a) and lake level increased (López-Blanco et al., 2024) (Fig. 4C, E, F) toward the Middle Holocene, a higher portion of heavier meltwater flowed into the lake and led to progressively enriched water. Additional contemporaneous and unpublished data directly retrieved from meltwater in Sierra Nevada showed highly negative values at the beginning of the melting (for example  $\delta^{18}\text{O} = -10.25$  in June 2020) and a progressive enrichment in heavier isotopes of meltwater ( $\delta^{18}\text{O} = -8.82$  in July 2020). Several studies have also provided evidence of progressive enrichment in heavy

isotopes in the liquid runoff during the melt season in both glacier and non-glacier sites (Penn et al., 2023; Taylor et al., 2001). Regional studies in Laguna Seca (Jiménez-Moreno et al., 2023b) and Padul (Camuera et al., 2019) also provided evidence of cold conditions around 15 cal kyr BP, possibly related to low summer insolation at that time (Laskar, 2004) (Fig. 4C). Biological activity was reduced here at LdRS by the low temperatures, as documented by the lowest numbers of diatoms (Llodrà-Llavrés et al., 2024), cladocerans (López-Blanco et al., 2024), and chironomids (Jiménez-Moreno et al., 2023a) encountered at this section in the LdRS sediment core. Steppic-like vegetation dominated by *Artemisia* and detritic sedimentation derived from early glacier melting were also key features of this section of the sediment core (Jiménez-Moreno et al., 2023a). Quantitative reconstructions based on membrane lipids (brGDGTs) also indicated low temperatures in a lower-elevation lake in the Sierra Nevada (Rodrigo-Gámiz et al., 2022).

The peak detected in the  $\delta^{18}\text{O}_{\text{ephippia}}$  around 7.2 cal kyr BP may be related to the existence of highly evaporated waters at the end of the summer, which were probably forced by higher spring and summer temperatures at the Holocene Thermal Maximum (HTM) in Sierra Nevada. This peak broadly agrees with the maximum in quantitative temperature inferences by chironomids (Jiménez-Moreno et al. 2023) and by branched glycerol dialkyl glycerol tetraether (brGDGTs) (Rodrigo-Gámiz et al. in preparation) from the same core. Seasonality was high in the Early Holocene, as reflected by the large differences between the winter and the summer insolation represented in Fig. 4C (Laskar et al. 2004). Here, precipitation and lake level were elevated (López-Blanco et al. 2024; Fig. 4F) but higher summer temperatures increased the summer evaporation and resulted on heavier oxygen isotopes in the early-autumn waters. According to our contemporaneous data, higher spring temperatures might have also contributed to an early thawing onset and a high  $\delta^{18}\text{O}_{\text{ephippia}}$  at the end of the ice-free season. In fact, coupled contemporaneous data of the spring and summer temperature and oxygen isotopic data during the four sampling years support this interpretation. In 2020, spring temperatures exhibited mean values of  $3.8^\circ\text{C}$ , which probably caused a delay in the thawing onset compared with 2022 and 2023, when the mean spring temperatures were  $5.7^\circ\text{C}$  and  $5.2^\circ\text{C}$ , respectively. An early thawing onset in 2022 and 2023 triggered by higher temperatures might explain the highly evaporated waters and high  $\delta^{18}\text{O}$  values at the end of the summer (Fig. 2). The amount of snow may have also had a secondary influence in the values observed in this part of the sedimentary record, expanding the effect of high temperatures on heavy isotope values when the snow mass was low, but moderating this outcome in a scenario of increased snow cover (see indicators of precipitation in Fig. 4E and 4F).

Minimum  $\delta^{18}\text{O}_{\text{ephippia}}$  values around 6.5 cal kyr BP may result from reduced summer temperatures and reduced seasonality (Fig. 4C, E), causing a delayed thawing and less evaporation in the summer and resulting in an opposite impact to that described above for enriched oxygen isotopes. Precipitation was still high at this time (Fig. 4F) and the high snow mass during this period might have further lowered the  $\delta^{18}\text{O}$ . Reduced summer temperatures around this period have been described in several quantitative reconstructions at local scales. Jiménez-Moreno et al., (2023a) inferred a rapid cooling of ca.  $1.5^\circ\text{C}$  in LdRS between 7.2 and 6.5 cal kyr BP whereas Rodrigo-Gámiz et al. (2022) also detected a temperature decline around 7.0 cal kyr BP in the Padul paleolake. At the regional scale and considering the insolation orbital forcing, different timings are expected derived from distinct patterns of summer/winter insolation at different latitudes. For the sake of example, quantitative reconstructions presented in Tarrats et al., (2018) also showed a summer temperature decline of  $1.5^\circ\text{C}$  but at 6.0 cal kyr BP in the Pyrenees ( $42^\circ\text{N}$ ).

### 5.2.2. After the 4.2 kyr event: Increasing Mediterranean influence and evaporation at lower lake levels

From 4.2 kyr BP onwards, there is a strong change in the tendency and the  $\delta^{18}\text{O}_{\text{ephippia}}$  signal exhibits an overall enrichment in absolute

values (Fig. 4D). This is probably caused by a source effect, which is the influence of moisture masses from different sources that have distinct  $\delta^{18}\text{O}$  values. In the Sierra Nevada, both the Atlantic Ocean and the Mediterranean Sea are important sources of atmospheric moisture (Fig. 1). Mediterranean waters are naturally more enriched (about 0.5 ‰–1 ‰) than the Atlantic, but additionally, the Atlantic moisture showed a gradual depletion in heavy isotopes during the sequential rainout as air masses travel from the source to the Sierra Nevada, exhibiting significantly lower oxygen isotope values compared to Mediterranean-derived precipitation (Araguas-Araguas and Tejeiro, 2005). The enrichment from 4.2 kyr BP onwards suggests a major role of the Mediterranean water as the main source of precipitation, which was probably amplified by a higher residence time and evaporation under a scenario of lower lake levels (Fig. 4E, F). Summer insolation decreases here and reconstructed temperatures during this period were lower (Jiménez-Moreno et al. 2023a; Rodrigo-Gámiz et al. in preparation) but evaporation was probably enhanced by the lower volume of the lake, as precipitation was reduced (López-Blanco et al. 2024; Fig. 4E). Toney et al. (2020) also recorded high  $\delta\text{D}_{\text{aq}}$  and  $\delta\text{D}_{\text{wax}}$  values in LdRS from this time onwards and inferred a major role of the precipitation source and amount of precipitation in the long-term signal. Notably, the  $\delta^{18}\text{O}_{\text{ephippia}}$  stratigraphy from 4.2 kyr BP onwards is highly concordant with the  $\delta\text{D}_{\text{aq}}$  (Fig. 4B, D), as both signals recorded the environmental source water used by aquatic plants and cladocerans. Multiple proxies having distinct environmental links agreed at inferring a drier stage and lower lake level from 5.0 cal kyr BP (Anderson et al., 2011; García-Alix et al., 2012; Jiménez-Espejo et al., 2014; Jiménez-Moreno and Anderson, 2012; López-Blanco et al., 2024), which might have also influenced the overall heavy isotopic signal detected from the 4.2 kyr BP event. The 4.2 kyr BP event was a phase of intense aridity caused by a significant weakening of the Atlantic Meridional Overturning Circulation (AMOC) and a southward shift of the Intertropical Convergence Zone (ITCZ) (Yan and Liu, 2019). A positive North Atlantic Oscillation (NAO)-like pattern in the atmosphere was also believed to be responsible for a drastic reduction in precipitation, mostly in the winter season (Bini et al., 2019 and references therein). Negative Western Mediterranean Oscillation (WeMO) conditions started to dominate the current climatic system in the southeastern Peninsula from this period onwards (Schirrmacher et al., 2020). WeMO is characterized by relatively warm and humid easterly winds and might have enhanced Mediterranean-sourced precipitation, resulting in high  $\delta^{18}\text{O}_{\text{ephippia}}$  in our sequence. Further evidence suggested shifts in the winter and Atlantic-sourced precipitation from the Early Holocene to a spring and more Mediterranean-derived rainfall in the Late Holocene (García-Alix et al., 2021; Toney et al., 2020; Zielhofer et al., 2017). Those changes are in phase with the overall enrichment of the  $\delta^{18}\text{O}$  signal in LdRS and with documented shifts in the dominance of modes of climatic variability (NAO/WeMO) in the past.

### 5.3. Methodological constraints

The taxon-specific approach used here has allowed the use of the chemical composition of ubiquitous chitinous invertebrates to go beyond the traditional approach consisting of fossil counting. The method is still constrained by the small size and weight of the chitinous remains, which limits the application of the method only to larger/heavy remains such as *Daphnia* ephippia. Technically, the application in smaller remains belonging to Chydoridae is possible, but the isolation of thousands of remains is required. Thus, sacrificing such a quantity of sediment only for this analysis does not seem a realistic scenario in most paleoecological studies. In sediment cores with high sedimentation rates and sufficient chitinous material, the  $\delta^{18}\text{O}_{\text{chitin}}$  from different taxa might provide distinct snapshots of the isotopic composition of the water throughout the year. For example, the low-resolution  $\delta^{18}\text{O}_{\text{Chydorus}}$  signal presented here probably reflects the isotopic composition of the water during the entire ice-free season, as carapaces of this taxon are formed during this period, in contrast with the  $\delta^{18}\text{O}_{\text{ephippia}}$ , which probably

represent the early autumn aquatic environment. Quantitative differences between both signals might be caused by seasonal changes but could also be ascribed to vital effects and the influence of other environmental parameters that need to be explored in the future.

## 6. Conclusions

Here we provide one of the first records describing past changes based on the oxygen isotopic composition of cladoceran ephippia in a well-studied lake sedimentary record in southern Iberia, where each data point is likely to represent the autumn  $\delta^{18}\text{O}$  water average of hundreds of years, assuming the current seasonal timing of ephippia production. Long-term changes in the  $\delta^{18}\text{O}$  stratigraphy are controlled by large-scale shifts in the dominance of distinct modes of climatic variability in the Sierra Nevada. The main change in our signal is coeval with the 4.2 kyr BP event, which separated generally depleted samples from those that are overall enriched. Depleted  $\delta^{18}\text{O}$  values between the deglaciation and 4.2 cal kyr BP correspond to the onset of Holocene warming and the predominance of Atlantic precipitation with oscillations triggered by the summer insolation. Highly depleted isotopic values followed by a general enrichment suggest a significant influence of Mediterranean-source precipitation after the 4.2 kyr BP, probably enhanced by arid conditions from 5.0 cal kyr BP. Minor oscillations within the two described periods were probably controlled by small-scale or local conditions. The detected patterns in ephippia  $\delta^{18}\text{O}$  appear to be largely consistent with the other independent paleoclimate proxies, suggesting that they most likely reflect broadscale hydrological changes.

Our research showed that oxygen isotope analysis in cladocerans is achievable in large remains, such as *Daphnia* resting eggs. Sorting out and getting isotopic signals in smaller cladocerans such as chydorids is technically feasible, but it takes a significant amount of effort and sediment, and probably results in a loss of resolution. Recognizing the potential of this application, more research is needed to fully understand the environmental controls on the cladoceran isotopic signal.

### CRediT authorship contribution statement

**Charo López-Blanco:** Writing – review & editing, Writing – original draft, Visualization, Project administration, Methodology, Investigation, Funding acquisition, Formal analysis, Data curation, Conceptualization. **Antonio García-Alix:** Writing – review & editing, Visualization, Validation, Supervision, Resources, Methodology, Investigation, Funding acquisition, Conceptualization. **Isabel Sánchez-Almazo:** Writing – review & editing, Visualization, Methodology, Investigation. **Gonzalo Jiménez-Moreno:** Writing – review & editing, Visualization, Validation, Resources, Investigation. **R.Scott Anderson:** Writing – review & editing, Validation, Investigation.

### Declaration of competing interest

The authors declare that they have no known competing financial interests or personal relationships that could have appeared to influence the work reported in this paper.

### Acknowledgments

This project has received funding from the European Union's Horizon 2020 research and innovation program under the Marie Skłodowska-Curie grant agreement No 892487 to CLB. This work has been also supported by the project PID2021-125619OB-C21 funded by Ministerio de Ciencia e Innovación/Agencia Estatal de Investigación/10.13039/501100011033/, by ERDF A way of making Europe / EU Union and by the research group RNM-190 (Junta de Andalucía). The authors thank two anonymous reviewers for their comments, which greatly improved the quality of this paper.

## References

- Anderson, R.S., Jiménez-Moreno, G., Carrión, J.S., Pérez-Martínez, C., 2011. Postglacial history of alpine vegetation, fire, and climate from Laguna de Río Seco, Sierra Nevada, southern Spain. *Quat. Sci. Rev.* 30, 1615–1629. <https://doi.org/10.1016/j.quascirev.2011.03.005>.
- Araguas-Araguas, L., Tejeiro, M., 2005. Isotope composition of precipitation and water vapour in the Iberian Peninsula. First results of the Spanish Network of isotopes in precipitation, in: *Isotopic Composition of Precipitation in the Mediterranean Basin in Relation to Air Circulation Patterns and Climate*. IAEA- TECDOC- 1453. pp. 173–190.
- Barea-Arco, J., Pérez-Martínez, C., Morales-Baquero, R., 2001. Evidence of a mutualistic relationship between an algal epibiont and its host, *Daphnia pulicaria*. *Limnol. Oceanogr.* 46, 871–881. <https://doi.org/10.4319/lo.2001.46.4.0871>.
- Beuning, K.R.M., Kelts, K., Ito, E., Johnson, T.C., 1997. Paleohydrology of Lake Victoria, East Africa, inferred from  $^{18}\text{O}/^{16}\text{O}$  ratios in sediment cellulose. *Geology* 25, 1083–1086. [https://doi.org/10.1130/0091-7613\(1997\)025<1083:POLVEA>2.3.CO;2](https://doi.org/10.1130/0091-7613(1997)025<1083:POLVEA>2.3.CO;2).
- Beuning, K.R.M., Kelts, K., Russell, J., Wolfe, B.B., 2002. Reassessment of Lake Victoria–Upper Nile River paleohydrology from oxygen isotope records of lake-sediment cellulose. *Geology* 30, 559–562. [https://doi.org/10.1130/0091-7613\(2002\)030<0559:ROLVUN>2.0.CO;2](https://doi.org/10.1130/0091-7613(2002)030<0559:ROLVUN>2.0.CO;2).
- Bini, M., Zanchetta, G., Perçou, A., Cartier, R., Català, A., Cacho, I., Dean, J.R., Di Rita, F., Drysdale, R.N., Finné, M., Isola, I., Jalali, B., Lirer, F., Magri, D., Masi, A., Marks, L., Mercuri, A.M., Peyron, O., Sadori, L., Sicre, M.A., Welc, F., Zielhofer, C., Brisset, E., 2019. The 4.2 ka BP Event in the Mediterranean region: An overview. *Clim. Past* 15, 555–577. <https://doi.org/10.5194/cp-15-555-2019>.
- Brodie, C., Kracht, O., Douthitt, C., 2016. EA-IRMS: Accurate and Precise Weight% O and  $\delta^{18}\text{O}$  Analysis of Nitrogen-rich Samples using the EA IsoLink IRMS System. *Appl. note Thermo Fish. Sci. Bremen, Ger.*
- Camuera, J., Jiménez-Moreno, G., Ramos-Román, M., García-Alix, A., Toney, J., Anderson, R., Jiménez-Espejo, F., Bright, J., Webster, C., Yanes, Y., Carrión, J., 2019. Vegetation and climate changes during the last two glacial-interglacial cycles in the western Mediterranean: A new long pollen record from Padul (southern Iberian Peninsula). *Quat. Sci. Rev.* 205, 86–105. <https://doi.org/10.1016/j.quascirev.2018.12.013>.
- Chang, J.C., Shulmeister, J., Gröcke, D.R., Woodward, C.A., 2018. Toward more accurate temperature reconstructions based on oxygen isotopes of subfossil chironomid head-capsules in Australia. *Limnol. Oceanogr.* 63, 295–307. <https://doi.org/10.1002/lno.10630>.
- Chang, J.C., Shulmeister, J., Woodward, C., Michalski, G., 2016. Can stable oxygen and hydrogen isotopes from Australian subfossil Chironomus head capsules be used as proxies for past temperature change? *J. Paleolimnol.* 56, 331–348. <https://doi.org/10.1007/s10933-016-9920-4>.
- Craig, H., 1961. Isotopic Variations in Meteoric Waters. *Science* 133, 1702–1703. <https://doi.org/10.1126/science.133.3465.1702>.
- Edgerton, B.A., Axford, Y., Chipman, M.L., 2024. Evaluating middle to late Holocene climate variability from  $\delta^{18}\text{O}$  of aquatic invertebrate remains in southwestern Greenland. *Quat. Sci. Rev.* 333, 108664. <https://doi.org/10.1016/j.quascirev.2024.108664>.
- Epstein, S., Thompson, P., Ya, C.J., Yapp, C., 1977. Oxygen and Hydrogen Isotope Ratios in Plant Cellulose. *Science* 198, 1209–1215.
- Frossard, V., Verneaux, V., Millet, L., Jenny, J., Arnaud, F., Magny, M., Perga, M., 2014. Reconstructing long-term changes (150 years) in the carbon cycle of a clear-water lake based on the stable carbon isotope composition ( $\delta^{13}\text{C}$ ) of chironomid and cladoceran subfossil remains. *Freshw. Biol.* 59, 789–802. <https://doi.org/10.1111/fwb.12304>.
- García-Alix, A., Camuera, J., Ramos-Román, M.J., Toney, J.L., Sachse, D., Schefuß, E., Jiménez-Moreno, G., Jiménez-Espejo, F.J., López-Avilés, A., Anderson, R.S., Yanes, Y., 2021. Paleohydrological dynamics in the Western Mediterranean during the last glacial cycle. *Glob. Planet. Change* 202, 103527. <https://doi.org/10.1016/j.gloplacha.2021.103527>.
- García-Alix, A., Jiménez-Moreno, G., Anderson, R.S., Jiménez Espejo, F.J., Delgado Huertas, A., 2012. Holocene environmental change in southern Spain deduced from the isotopic record of a high-elevation wetland in Sierra Nevada. *J. Paleolimnol.* 48, 471–484. <https://doi.org/10.1007/s10933-012-9625-2>.
- Griffiths, K., Michelutti, N., Blais, J., Kimpe, L., Smol, J., 2010. Comparing nitrogen isotopic signals between bulk sediments and invertebrate remains in high Arctic seabird-influenced ponds. *J. Paleolimnol.* 44, 405–412. <https://doi.org/10.1007/s10933-009-9354-3>.
- Heiri, O., Schilder, J., Van Hardenbroek, M., 2012. Stable isotopic analysis of fossil chironomids as an approach to environmental reconstruction: State of development and future challenges. *Fauna nor.* 31, 7–18. <https://doi.org/10.5324/fn.v31i0.1436>.
- Holtvoeth, J., Whiteside, J.H., Engels, S., Freitas, F.S., Grice, K., Greenwood, P., Johnson, S., Kendall, I., Lenggler, S.K., Lücke, A., Mayr, C., Naafs, B.D.A., Rohrsen, M., Sepúlveda, J., 2019. The paleolimnologist's guide to compound-specific stable isotope analysis – An introduction to principles and applications of CSIA for Quaternary lake sediments. *Quat. Sci. Rev.* 207, 101–133. <https://doi.org/10.1016/j.quascirev.2019.01.001>.
- Janssen, R., Vincken, J., van den Broek, L., Fogliano, V., Lakemond, C., 2017. Nitrogen-to-Protein Conversion Factors for Three Edible Insects: *Tenebrio molitor*, *Alphitobius diaperinus*, and *Hermetia illucens*. *J. Agric. Food Chem.* 65, 2275–2278.
- Jiménez-Espejo, F.J., García-Alix, A., Jiménez-Moreno, G., Rodrigo-Gámiz, M., Anderson, R.S., Rodríguez-Tovar, F.J., Martínez-Ruiz, F., Giralt, S., Delgado Huertas, A., Pardo-Igúzquiza, E., 2014. Saharan aeolian input and effective humidity variations over western Europe during the Holocene from a high altitude record. *Chem. Geol.* 374–375, 1–12. <https://doi.org/10.1016/j.chemgeo.2014.03.001>.
- Jiménez-Moreno, G., Anderson, R.S., 2012. Holocene vegetation and climate change recorded in alpine bog sediments from the Borreguiles de la Virgen, Sierra Nevada, southern Spain. *Quat. Res.* 77, 44–53. <https://doi.org/10.1016/j.yqres.2011.09.006>.
- Jiménez-Moreno, G., Heiri, O., García-Alix, A., Anderson, R.S., Jiménez-Espejo, F.J., López-Blanco, C., Jiménez, L., Pérez-Martínez, C., Rodrigo-Gámiz, M., López-Avilés, A., Camuera, J., 2023a. Holocene summer temperature reconstruction based on a chironomid record from Sierra Nevada, southern Spain. *Quat. Sci. Rev.* 319. <https://doi.org/10.1016/j.quascirev.2023.108343>.
- Jiménez-Moreno, G., López-Avilés, A., García-Alix, A., Ramos-Román, M.J., Camuera, J., Mesa-Fernández, J.M., Jiménez-Espejo, F.J., López-Blanco, C., Carrión, J.S., Anderson, R.S., 2023b. Laguna Seca sediments reveal environmental and climate change during the latest Pleistocene and Holocene in Sierra Nevada, southern Iberian Peninsula. *Palaeogeogr. Palaeoclimatol. Palaeoecol.* 631. <https://doi.org/10.1016/j.palaeo.2023.111834>.
- Lasher, G.E., Axford, Y., McFarlin, J.M., Kelly, M.A., Osterberg, E.C., Berkelhammer, M. B., 2017. Holocene temperatures and isotopes of precipitation in Northwest Greenland recorded in lacustrine organic materials. *Quat. Sci. Rev.* 170, 45–55. <https://doi.org/10.1016/j.quascirev.2017.06.016>.
- Laskar, J., 2004. Long-term solution for the insolation quantities of the Earth. *Proc. Int. Astron. Union* 2, 465. <https://doi.org/10.1017/S1743921307011404>.
- Leng, M., Lamb, A., Heaton, T., Marshall, J., Wolfe, Brent, B., Jones, M., Holmes, J., Arrowsmith, C., 2006. Isotopes in lake sediments. Volume 10, Developments in Paleoenvironmental Research. doi: 10.1007/1-4020-2504-1\_04.
- Leng, M.J., Marshall, J.D., 2004. Palaeoclimate interpretation of stable isotope data from lake sediment archives. *Quat. Sci. Rev.* 23, 811–831. <https://doi.org/10.1016/j.quascirev.2003.06.012>.
- Liu, J., Cheng, L., Liu, Q., Yao, S., Wang, X., Liu, Y., Zhang, Y., Xue, B., 2023. Sedimentary macrophyte  $\delta^{13}\text{C}$  cellulose record of environmental evolution over the past century in East Taihu Lake, China. *Ecol. Indic.* 154, 110716. <https://doi.org/10.1016/j.ecolind.2023.110716>.
- Llodrà-Llavrés, J., Jiménez-Moreno, G., García-Alix, A., Anderson, R.S., Jiménez-Espejo, F.J., López-Blanco, C., Rodrigo-Gámiz, M., Pérez-Martínez, C., 2024. Holocene paleoenvironmental and paleoclimatic variability in a high mountain lake in Sierra Nevada (Spain): insights from diatom analysis. *Quaternary Science Reviews* 334. <https://doi.org/10.1016/j.quascirev.2024.108984>.
- López-Blanco, C., García-Alix, A., Jiménez-Moreno, G., Rodrigo-Gámiz, M., Anderson, R. S., 2024. Climatic fluctuations over the Holocene in southern Iberia (Sierra Nevada, Spain) reconstructed by fossil cladocerans. *Palaeogeogr. Palaeoclimatol. Palaeoecol.* 638. <https://doi.org/10.1016/j.palaeo.2023.111989>.
- Mayr, C., Laprida, C., Lücke, A., Martín, R.S., Massafero, J., Ramón-Mercu, J., Wissel, H., 2015. Oxygen isotope ratios of chironomids, aquatic macrophytes and ostracods for lake-water isotopic reconstructions - Results of a calibration study in Patagonia. *J. Hydrol.* 529, 600–607. <https://doi.org/10.1016/j.jhydrol.2014.11.001>.
- Morales-Baquero, R., Carrillo, P., Barea-Arco, J., Pérez-Martínez, C., Villar-Ariza, M., 2006. Climate-driven changes on phytoplankton-zooplankton coupling and nutrient availability in high mountain lakes of Southern Europe. *Freshw. Biol.* 51, 989–998. <https://doi.org/10.1111/j.1365-2427.2006.01545.x>.
- Moreno, A., Sancho, C., Bartolomé, M., Oliva-Urcia, B., Delgado-Huertas, A., Estrela, M. J., Corell, D., López-Moreno, J.I., Cacho, I., 2014. Climate controls on rainfall isotopes and their effects on cave drip water and speleothem growth: The case of Molinos cave (Teruel, NE Spain). *Clim. Dyn.* 43, 221–241. <https://doi.org/10.1007/s00382-014-2140-6>.
- Penn, K., Marshall, S.J., Sinclair, K.E., 2023. Seasonal enrichment of heavy isotopes in meltwater runoff from Haig Glacier, Canadian Rocky Mountains. *Front. Earth Sci.* 11, 1–14. <https://doi.org/10.3389/feart.2023.1125877>.
- Pérez-Martínez, C., Barea-Arco, J., Conde-Porcuna, J.M., Morales-Baquero, R., 2007. Reproduction strategies of *Daphnia pulicaria* population in a high mountain lake of Southern Spain. *Hydrobiologia* 594, 75–82. <https://doi.org/10.1007/s10750-007-9084-3>.
- Perga, M.E., 2010. Potential of  $\delta^{13}\text{C}$  and  $\delta^{15}\text{N}$  of cladoceran subfossil exoskeletons for paleo-ecological studies. *J. Paleolimnol.* 44, 387–395. <https://doi.org/10.1007/s10933-009-9340-9>.
- Perga, M.E., Gerdeux, D., 2006. Seasonal variability in the  $\delta^{13}\text{C}$  and  $\delta^{15}\text{N}$  values of the zooplankton taxa in two alpine lakes. *Acta Oecologica* 30, 69–77. <https://doi.org/10.1016/j.actao.2006.01.007>.
- Raposeiro, P.M., Ritter, C., Abbott, M., Hernandez, A., Pimentel, A., Lasher, E., Plóciennik, M., Berljolli, V., Kotrys, B., Pombal, X.P., Souto, M., Giralt, S., Gonçalves, V., 2024. Late Holocene climate dynamics in the Azores archipelago. *Quat. Sci. Rev.* 331. <https://doi.org/10.1016/j.quascirev.2024.108617>.
- Rodrigo-Gámiz, M., García-Alix, A., Jiménez-Moreno, G., Ramos-Román, M.J., Camuera, J., Toney, J.L., Sachse, D., Anderson, R.S., Sinnighe Damsté, J.S., 2022. Paleoclimate reconstruction of the last 36 kyr based on branched glycerol dialkyl glycerol tetraethers in the Padul palaeolake record (Sierra Nevada, southern Iberian Peninsula). *Quat. Sci. Rev.* 281. <https://doi.org/10.1016/j.quascirev.2022.107434>.
- Schilder, J., Bastviken, D., van Hardenbroek, M., Leuenberger, M., Rinta, P., Stötter, T., Heiri, O., 2015. The stable carbon isotopic composition of *Daphnia ephippia* in small, temperate lakes reflects in-lake methane availability. *Limnol. Oceanogr.* 60, 1064–1075. <https://doi.org/10.1002/lno.10079>.
- Schilder, J., Van Hardenbroek, M., Bodelier, P., Kirilova, E., Leuenberger, M., Lotter, A., Heiri, O., 2017. Trophic state changes can affect the importance of methane-derived carbon in aquatic food webs. *Proc. r. Soc. B Biol. Sci.* 284, 20170278. <https://doi.org/10.1098/rspb.2017.0278>.

- Sterngber, L., DeNiro, M., 1963. Isotopic Composition of Cellulose from C3, C4 and CAM plants growing near one another. *Science* 220, 947–949.
- Schirmacher, J., Andersen, N., Schneider, R.R., Weinelt, M., 2020. Fossil leaf wax hydrogen isotopes reveal variability of Atlantic and Mediterranean climate forcing on the southeast Iberian Peninsula between 6000 to 3000 cal. BP. *PLoS One* 15, 1–19. <https://doi.org/10.1371/journal.pone.0243662>.
- Sternberg, L., Deniro, M.J., Keeley, J.E., 1984. Hydrogen, oxygen, and carbon isotope ratios of cellulose from submerged aquatic crassulacean acid metabolism and non-crassulacean acid metabolism plants. *Plant Physiol.* 76, 68–70. <https://doi.org/10.1104/pp.76.1.68>.
- Sternberg, L.D.S.L., Deniro, M.J., Sloan, M.E., Black, C.C., 1986. Compensation Point and Isotopic Characteristics of C3 /C4 Intermediates and Hybrids in *Panicum*. *Plant Physiol.* 80, 242–245. <https://doi.org/10.1104/pp.80.1.242>.
- Street-Perrott, F.A., Holmes, J.A., Robertson, I., Ficken, K.J., Koff, T., Loader, N.J., Marshall, J.D., Martma, T., 2018. The Holocene isotopic record of aquatic cellulose from Lake Äntu Sinijärvi, Estonia: Influence of changing climate and organic-matter sources. *Quat. Sci. Rev.* 193, 68–83. <https://doi.org/10.1016/j.quascirev.2018.05.010>.
- Taylor, S., Feng, X., Kirchner, J.W., Osterhuber, R., Klaue, B., Renshaw, C.E., 2001. Isotopic evolution of a seasonal snowpack and its melt. *Water Resour. Res.* 37, 759–769. <https://doi.org/10.1029/2000WR900341>.
- Toney, J., García-Alix, A., Jiménez-Moreno, G., Anderson, R., Moossen, H., Seki, O., 2020. New insights into Holocene hydrology and temperature from lipid biomarkers in western Mediterranean alpine wetlands. *Quat. Sci. Rev.* 240, 106395. <https://doi.org/10.1016/j.quascirev.2020.106395>.
- Tracey, M.V., 1955. *Analysis*. 264–274.
- van Hardenbroek, M., Chakraborty, A., Davies, K.L., Harding, P., Heiri, O., Henderson, A. C.G., Holmes, J.A., Lasher, G.E., Leng, M.J., Panizzo, V.N., Roberts, L., Schilder, J., Trueman, C.N., Wooller, M.J., 2018. The stable isotope composition of organic and inorganic fossils in lake sediment records: Current understanding, challenges, and future directions. *Quat. Sci. Rev.* 196, 154–176. <https://doi.org/10.1016/j.quascirev.2018.08.003>.
- van Hardenbroek, M., Gröcke, D.R., Sauer, P.E., Elias, S.A., 2012. North American transect of stable hydrogen and oxygen isotopes in water beetles from a museum collection. *J. Paleolimnol.* 48, 461–470. <https://doi.org/10.1007/s10933-012-9623-4>.
- Verbruggen, F., Heiri, O., Reichart, G.J., Blaga, C., Lotter, A.F., 2011. Stable oxygen isotopes in chironomid and cladoceran remains as indicators for lake-water  $\delta^{18}\text{O}$ . *Limnol. Oceanogr.* 56, 2071–2079. <https://doi.org/10.4319/lo.2011.56.6.2071>.
- Verbruggen, F., Heiri, O., Reichart, G.J., de Leeuw, J.W., Nierop, K.G.J., Lotter, A.F., 2010a. Effects of chemical pretreatments on  $\delta^{18}\text{O}$  measurements, chemical composition, and morphology of chironomid head capsules. *J. Paleolimnol.* 43, 857–872. <https://doi.org/10.1007/s10933-009-9374-z>.
- Verbruggen, F., Heiri, O., Reichart, G.J., Lotter, A.F., 2010b. Chironomid  $\delta^{18}\text{O}$  as a proxy for past lake water  $\delta^{18}\text{O}$ : a Lateglacial record from Rotsee (Switzerland). *Quat. Sci. Rev.* 29, 2271–2279. <https://doi.org/10.1016/j.quascirev.2010.05.030>.
- Wooller, M., Francis, D., Fogel, M., Miller, G.H., Walker, I., Wolfe, A., 2004. Quantitative paleotemperature estimates from  $\delta^{18}\text{O}$  of chironomid head capsules preserved in arctic lake sediments. *J. Paleolimnol.* 31. <https://doi.org/10.1023/B:1365-3040.1992.tb01652.x>.
- Yakir, D., 1992. Variations in the natural abundance of oxygen-18 and deuterium in plant carbohydrates. *Plant. Cell Environ.* 15, 1005–1020. <https://doi.org/10.1111/j.1365-3040.1992.tb01652.x>.
- Yan, M., Liu, J., 2019. Physical processes of cooling and mega-drought during the 4.2 ka BP event: Results from TraCE-21ka simulations. *Clim. past* 15, 265–277. <https://doi.org/10.5194/cp-15-265-2019>.
- Zielhofer, C., Fletcher, W.J., Mischke, S., De Batist, M., Campbell, J.F.E., Joannin, S., Tjallingii, R., El Hamouti, N., Junginger, A., Steele, A., Bussmann, J., Schneider, B., Lauer, T., Spitzer, K., Strupler, M., Brachert, T., Mikdad, A., 2017. Atlantic forcing of Western Mediterranean winter rain minima during the last 12,000 years. *Quat. Sci. Rev.* 157, 29–51. <https://doi.org/10.1016/j.quascirev.2016.11.037>.